Influence of the even-odd effect on the crystal structure, band structure and optical properties of hybrid crystals of the H_3N-$(CH_2)_n$-NH_3PbX_4 (n=4-8, X=Cl, Br, I) type

M.I. Balanov[1,2,3], A.V. Emeline[3], D.S. Shtarev[1,2*]

[1] – *Department of Materials Science, Shenzhen MSU-BIT University, PRC*

[2] – *Institute of High Technologies and Advanced Materials of the Far Eastern Federal University, Vladivostok, Russia*

[3] *Saint-Petersburg State University, Laboratory 'Photonics of crystals', St.-Petersburg, Russia.*

[*] *Corresponding author's e-mail:* shtarev@mail.ru

Supplementary materials

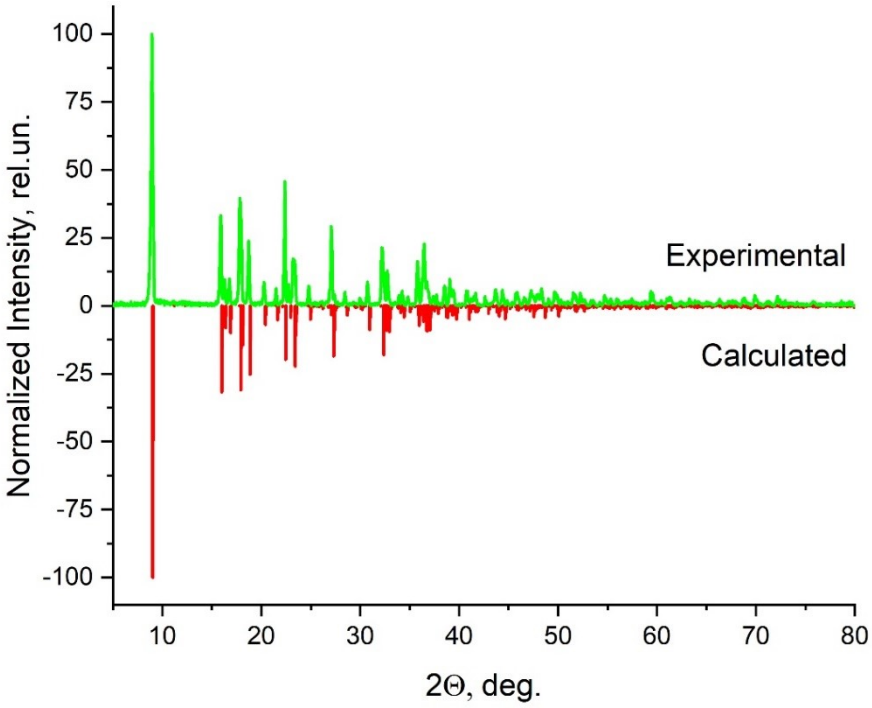

Figure S1. Powder X-ray diffraction pattern of the hybrid crystal $(C_4)DAPbCl_4$ (green line at top) compared to that calculated from the known structure (CCDC # 1501643, red line at bottom).

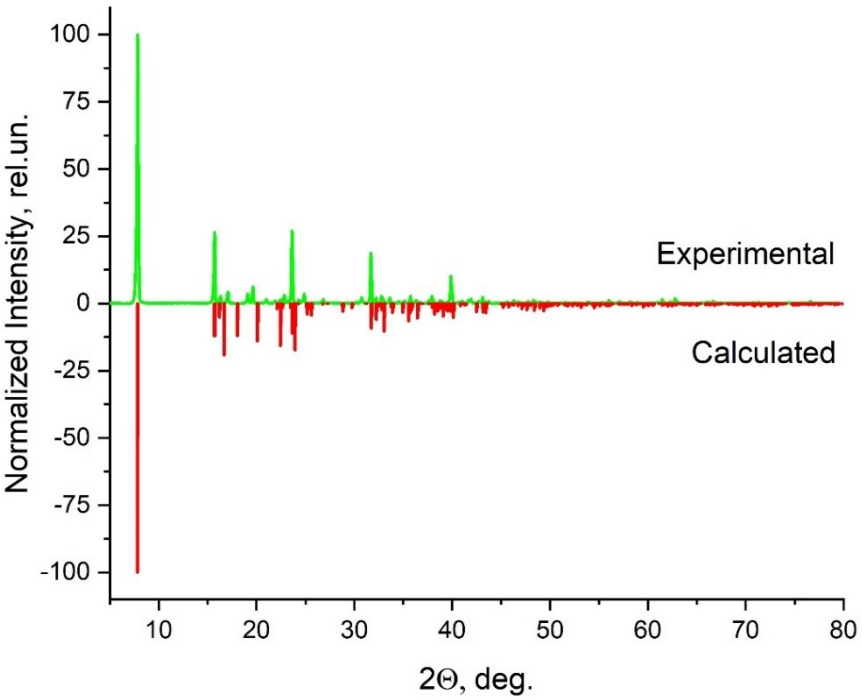

Figure S2. Powder X-ray diffraction pattern of the hybrid crystal $(C_5)DAPbCl_4$ (green line at top) compared to that calculated from the known structure ([14], red line at bottom).

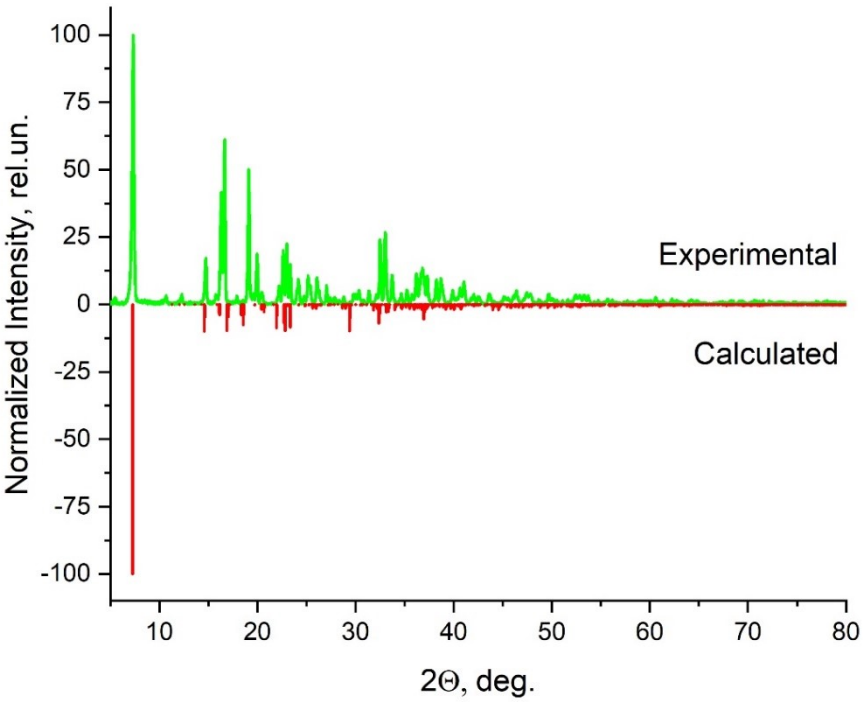

Figure S3. Powder X-ray diffraction pattern of the hybrid crystal $(C_6)DAPbCl_4$ (green line at top) compared to that calculated from the known structure ([13], red line at bottom).

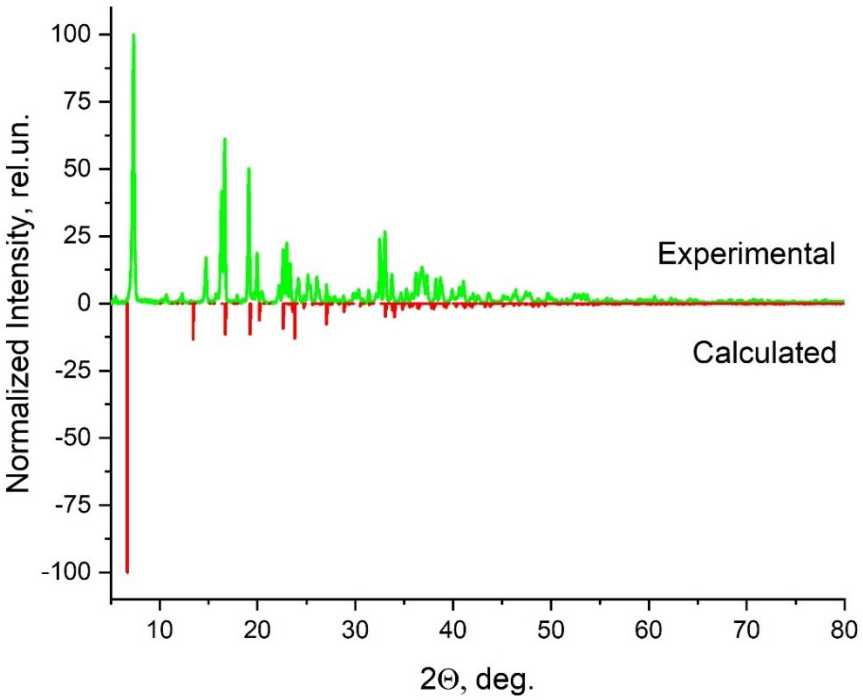

Figure S4. Powder X-ray diffraction pattern of the hybrid crystal $(C_7)DAPbCl_4$ (green line at top) compared to that calculated from structural data obtained in current study (red line at bottom).

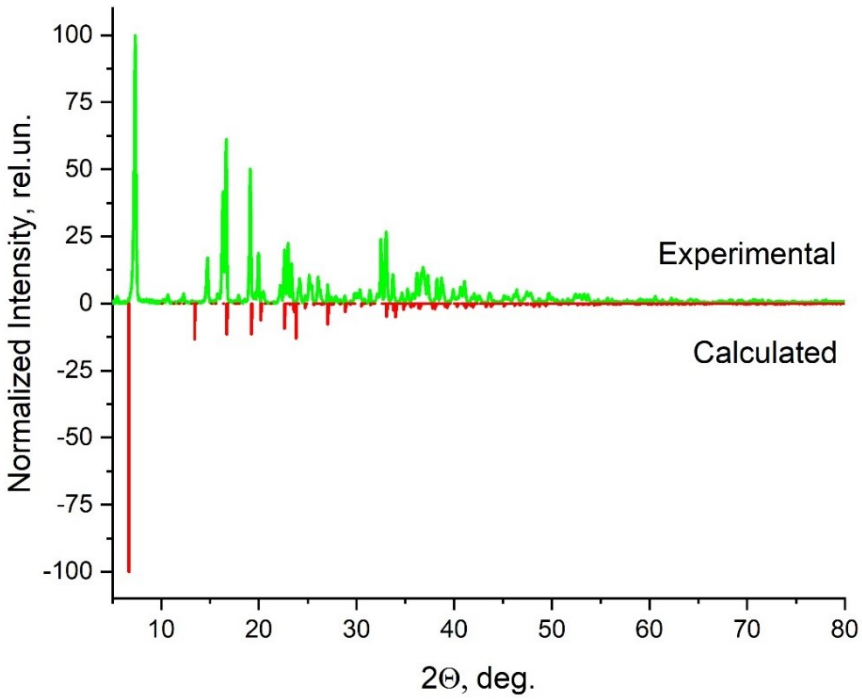

Figure S5. Powder X-ray diffraction pattern of the hybrid crystal $(C_8)DAPbCl_4$ (green line at top) compared to that calculated from structural data obtained in current study (red line at bottom).

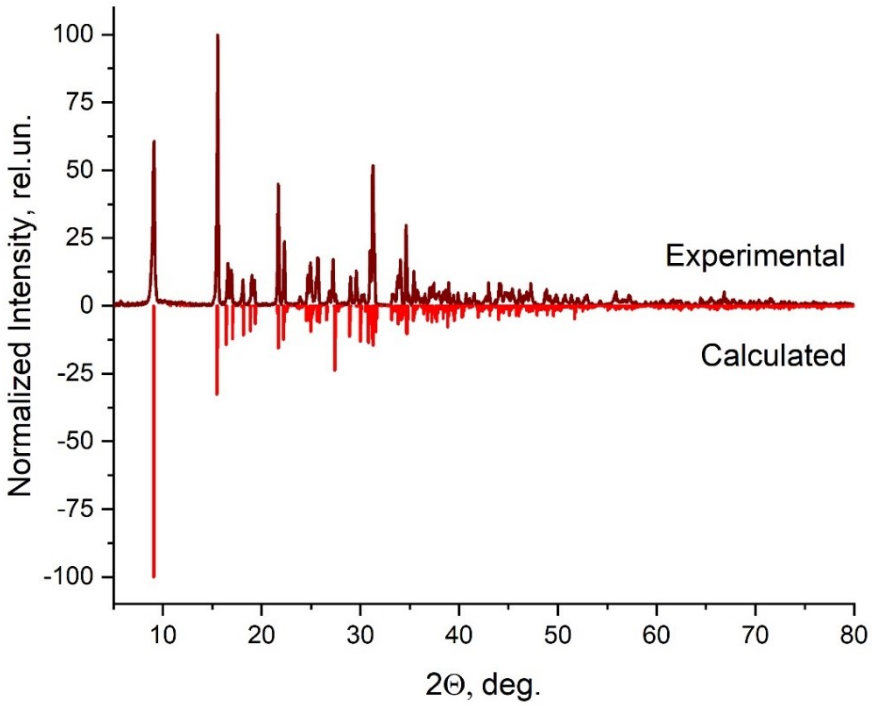

Figure S6. Powder X-ray diffraction pattern of the hybrid crystal $(C_4)DAPbBr_4$ (dark-red line at top) compared to that calculated from the known structure (CCDC # 1545802, red line at bottom).

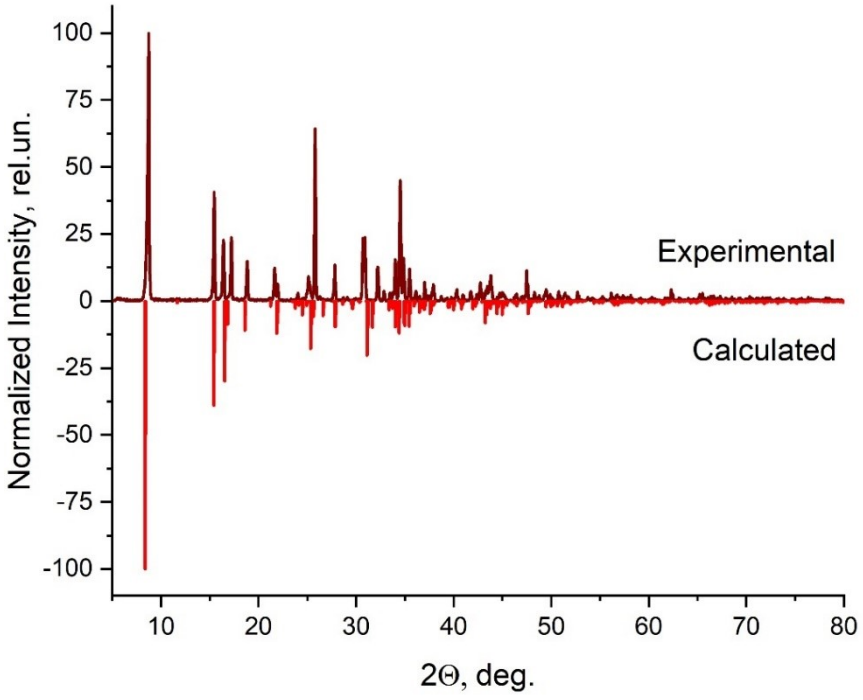

Figure S7. Powder X-ray diffraction pattern of the hybrid crystal $(C_5)DAPbBr_4$ (dark-red line at top) compared to that calculated from the known structure ([14], red line at bottom).

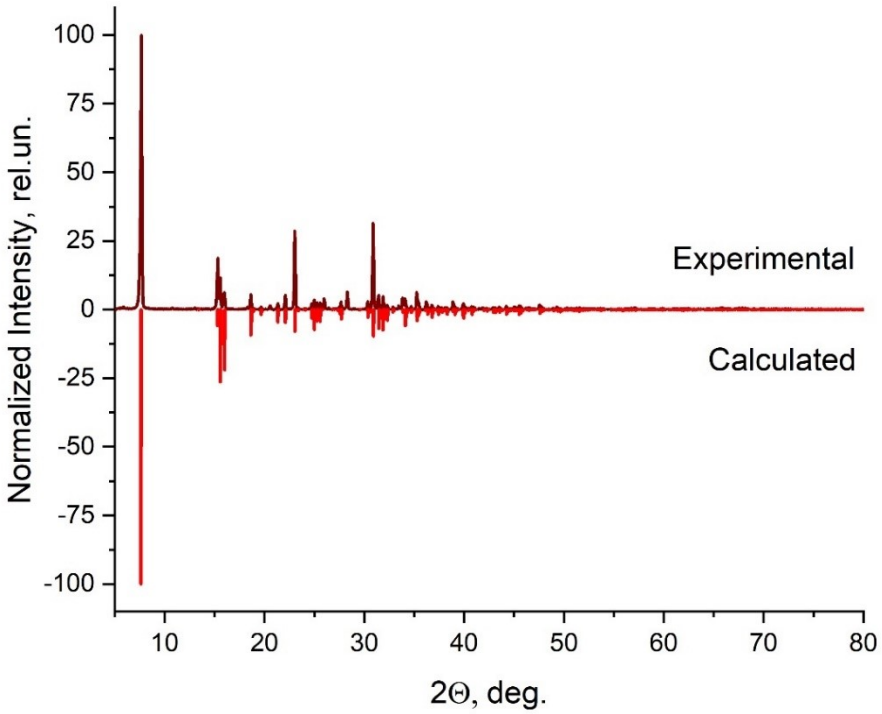

Figure S8. Powder X-ray diffraction pattern of the hybrid crystal $(C_6)DAPbBr_4$ (dark-red line at top) compared to that calculated from the known structure (CCDC # 7203880, red line at bottom).

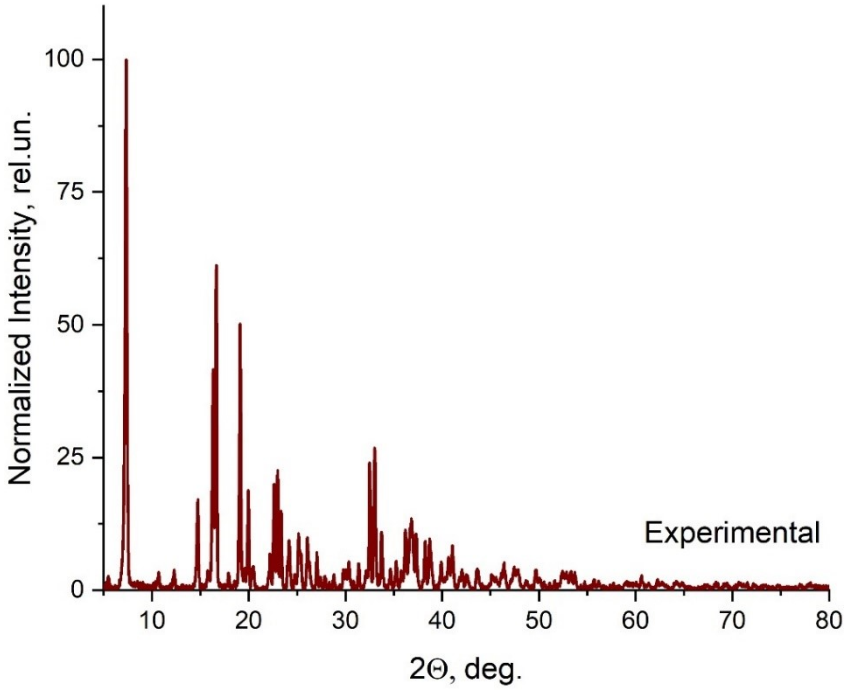

Figure S9. Powder X-ray diffraction pattern of the hybrid crystal $(C_7)DAPbBr_4$

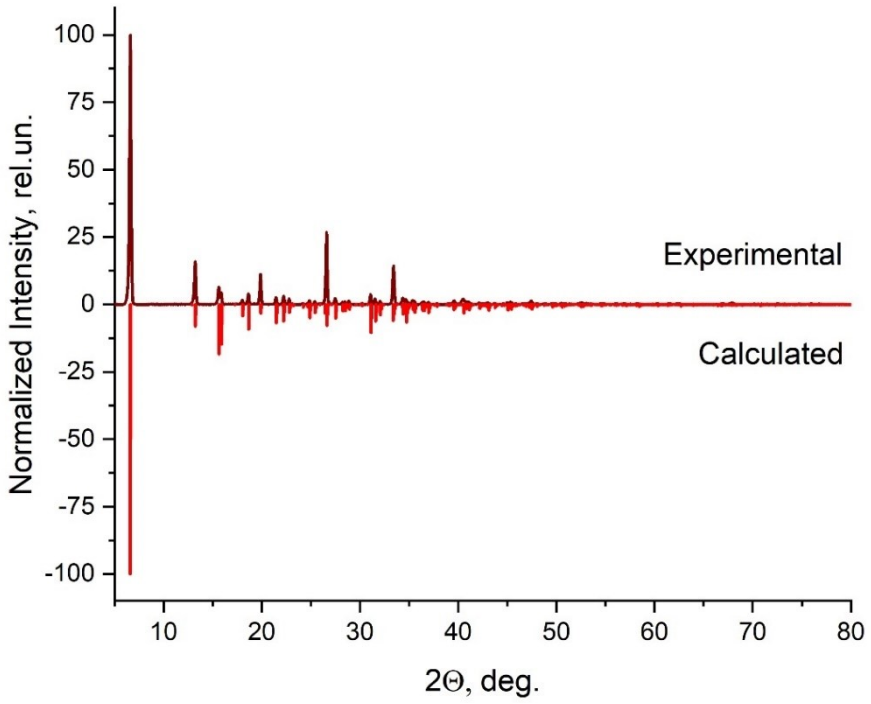

Figure S10. Powder X-ray diffraction pattern of the hybrid crystal $(C_8)DAPbBr_4$ (dark-red line at top) compared to that calculated from the known structure (CCDC # 1545806, red line at bottom).

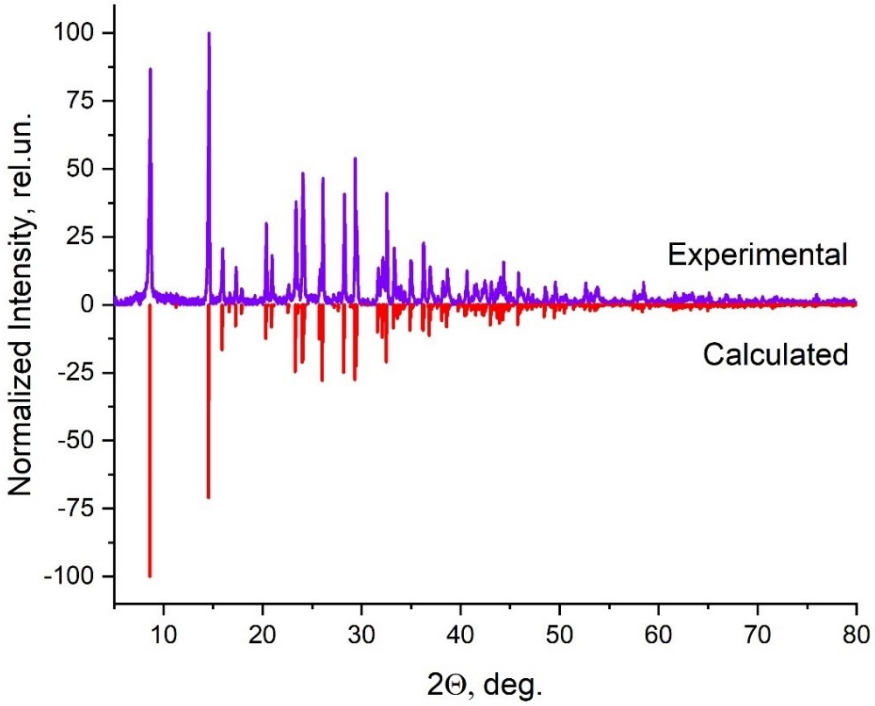

Figure S11. Powder X-ray diffraction pattern of the hybrid crystal $(C_4)DAPbI_4$ (purple line at top) compared to that calculated from the known structure (CCDC # 7207475, red line at bottom).

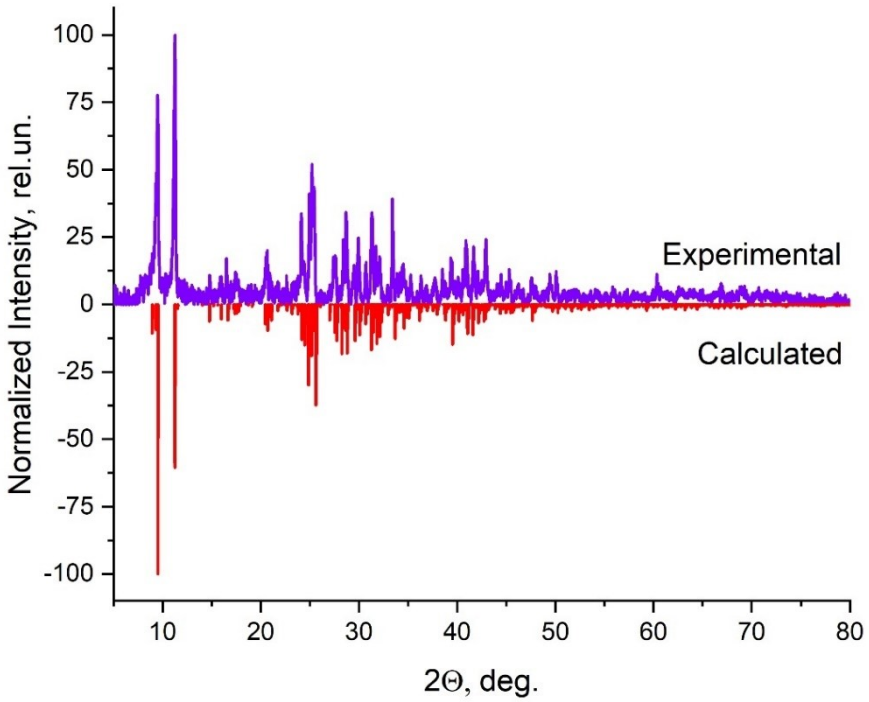

Figure S12. Powder X-ray diffraction pattern of the hybrid crystal $(C_5)DAPbI_4$ (purple line at top) compared to that calculated from the known structure ([14], red line at bottom).

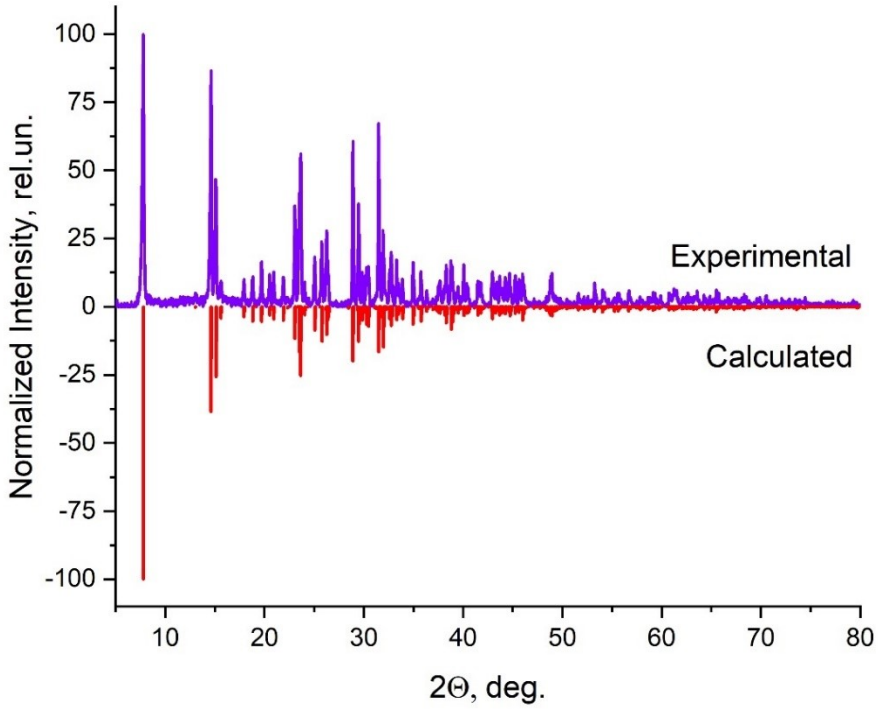

Figure S13. Powder X-ray diffraction pattern of the hybrid crystal $(C_6)DAPbI_4$ (purple line at top) compared to that calculated from the known structure (CCDC # 7203879, red line at bottom).

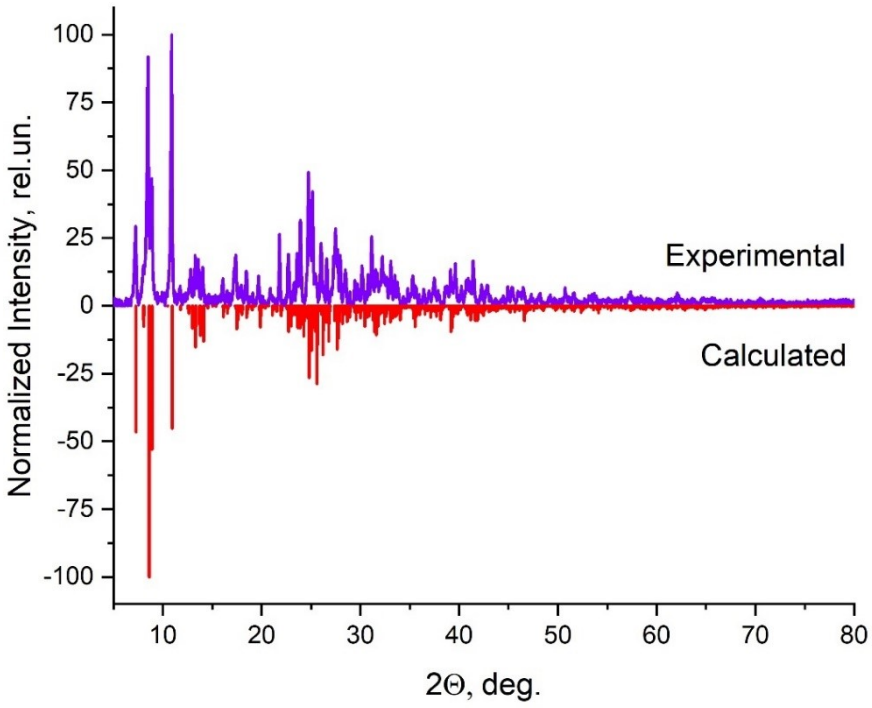

Figure S14. Powder X-ray diffraction pattern of the hybrid crystal $(C_7)DAPbI_4$ (purple line at top) compared to that calculated from the known structure (CCDC # 7207476, red line at bottom).

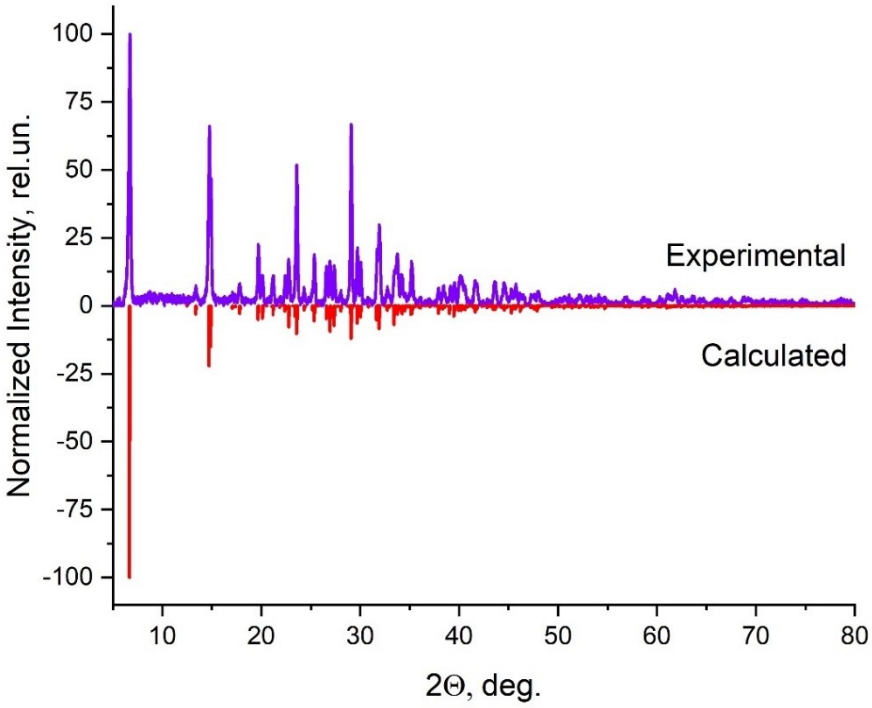

Figure S15. Powder X-ray diffraction pattern of the hybrid crystal $(C_8)DAPbI_4$ (purple line at top) compared to that calculated from the known structure (CCDC # 7207477, red line at bottom).

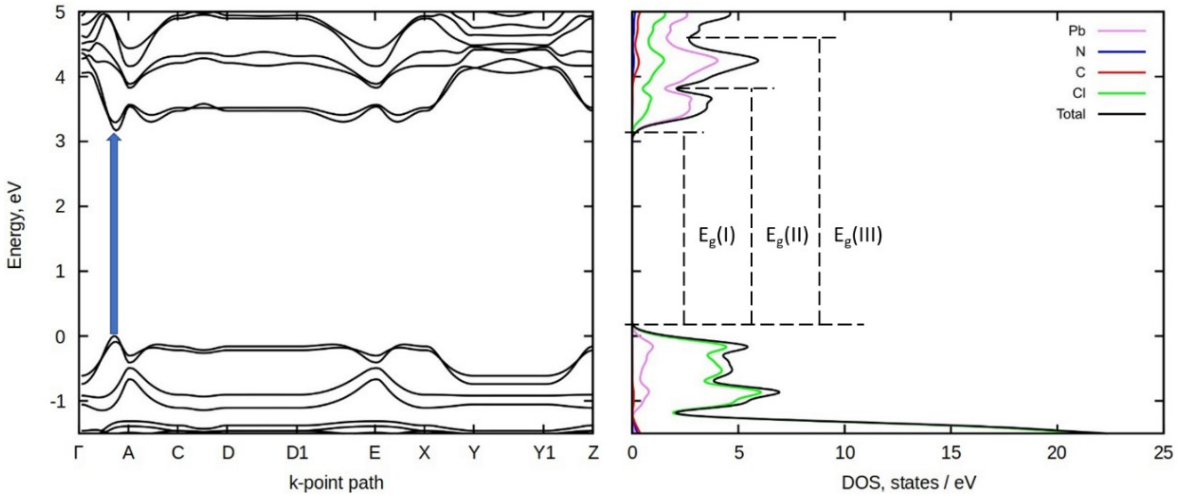

Figure S16. Electronic band structure (left) and density of states (right) for a $(C_5)DAPbCl_4$ hybrid crystal. The blue arrow indicates the electronic transition between the top of the valence band and the bottom of the conduction band.

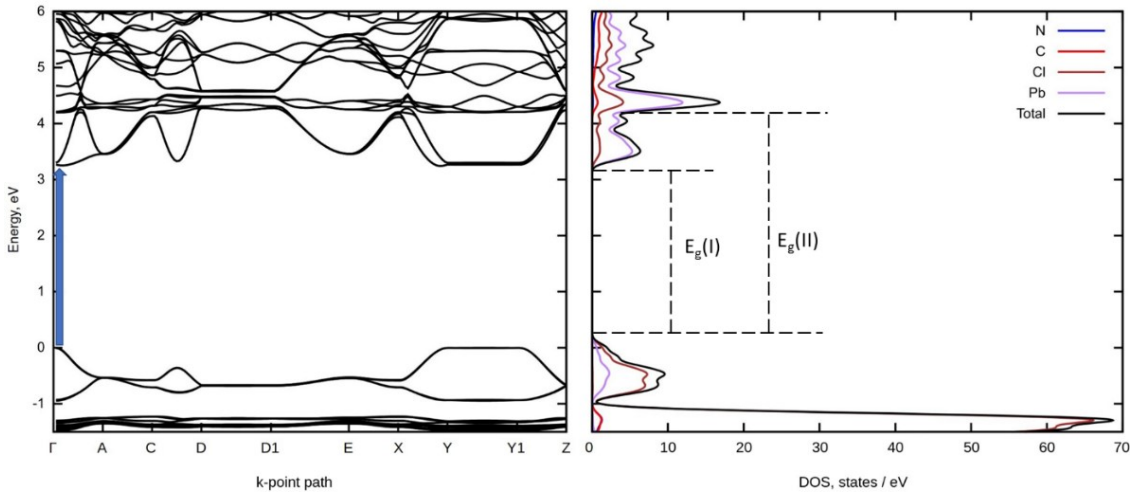

Figure S17. Electronic band structure (left) and density of states (right) for a $(C_6)DAPbCl_4$ hybrid crystal. The blue arrow indicates the electronic transition between the top of the valence band and the bottom of the conduction band.

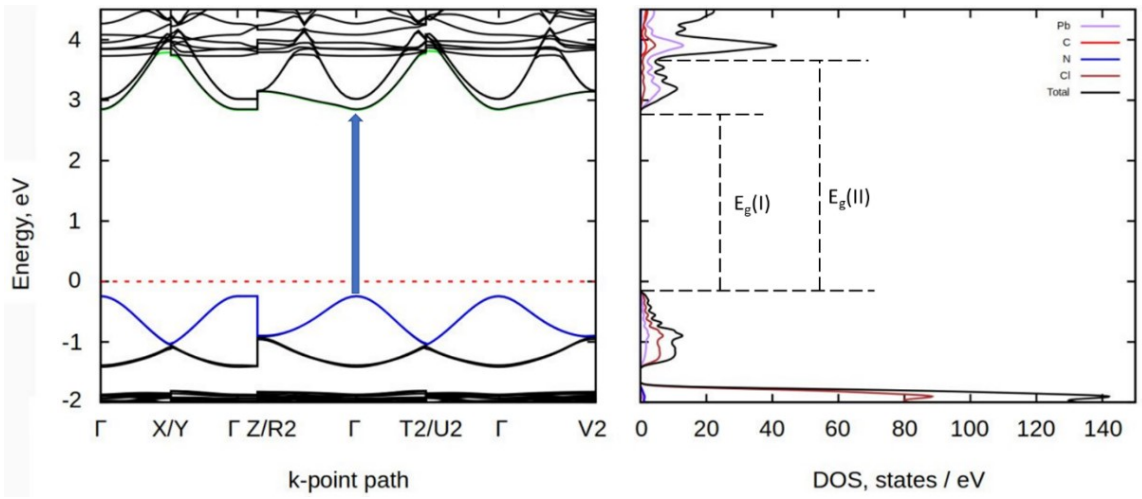

Figure S18. Electronic band structure (left) and density of states (right) for a $(C_7)DAPbCl_4$ hybrid crystal. The blue arrow indicates the electronic transition between the top of the valence band and the bottom of the conduction band.

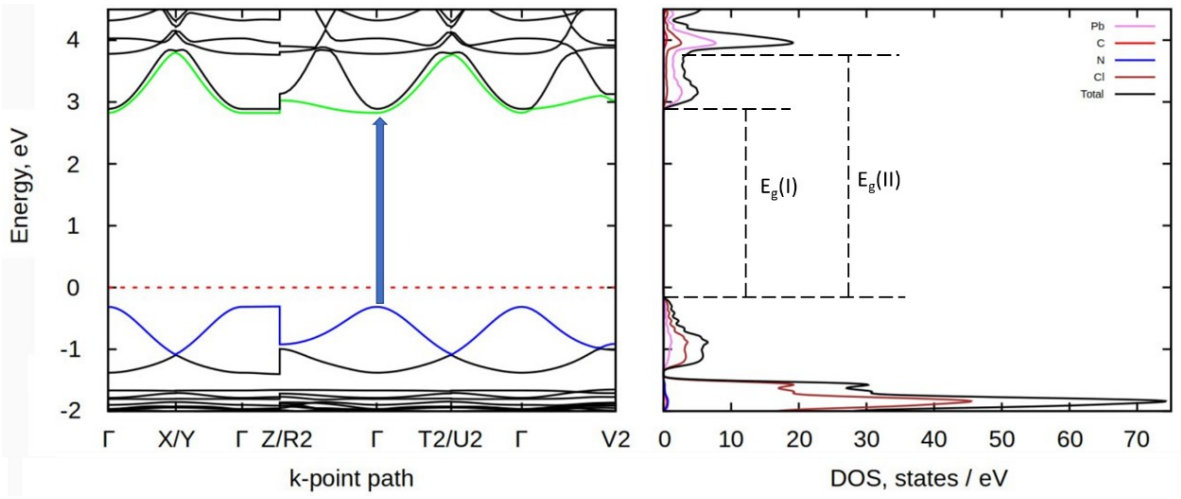

Figure S19. Electronic band structure (left) and density of states (right) for a $(C_8)DAPbCl_4$ hybrid crystal. The blue arrow indicates the electronic transition between the top of the valence band and the bottom of the conduction band.

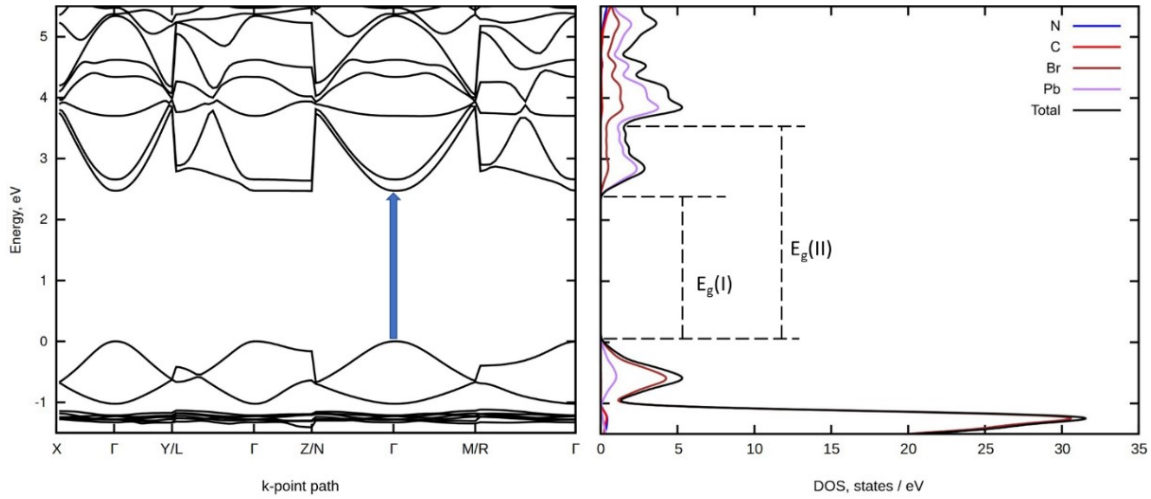

Figure S20. Electronic band structure (left) and density of states (right) for a $(C_4)DAPbBr_4$ hybrid crystal. The blue arrow indicates the electronic transition between the top of the valence band and the bottom of the conduction band.

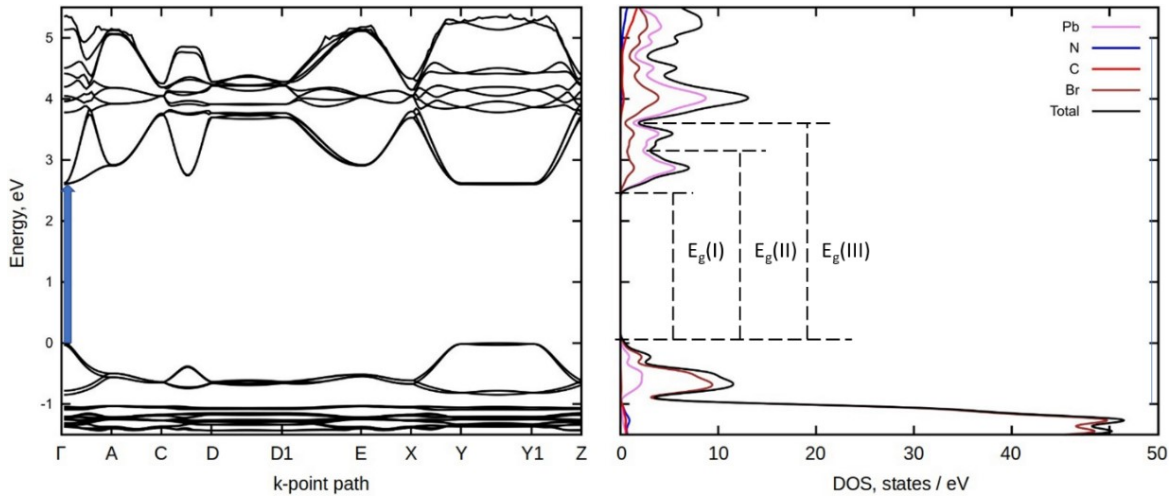

Figure S21. Electronic band structure (left) and density of states (right) for a $(C_5)DAPbBr_4$ hybrid crystal. The blue arrow indicates the electronic transition between the top of the valence band and the bottom of the conduction band.

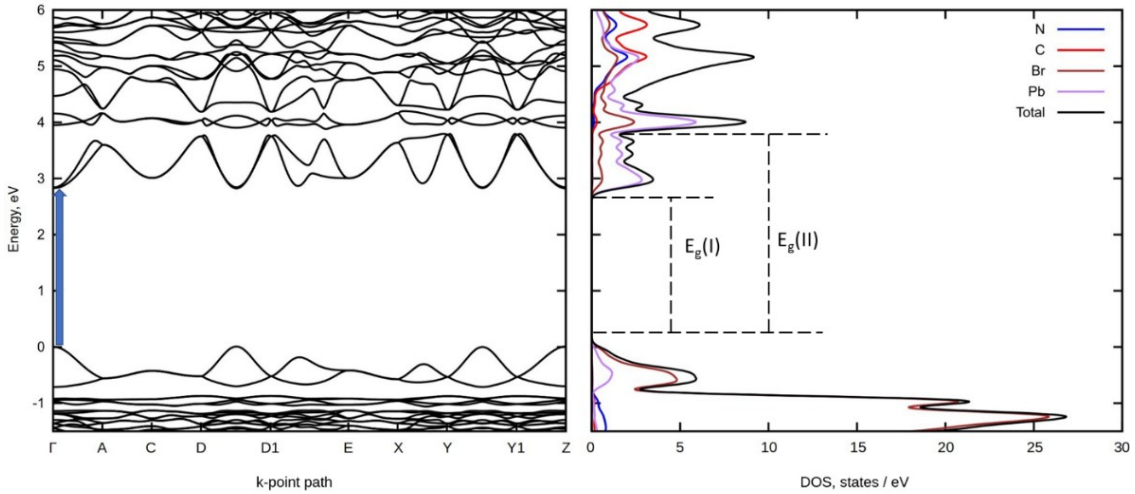

Figure S22. Electronic band structure (left) and density of states (right) for a $(C_6)DAPbBr_4$ hybrid crystal. The blue arrow indicates the electronic transition between the top of the valence band and the bottom of the conduction band.

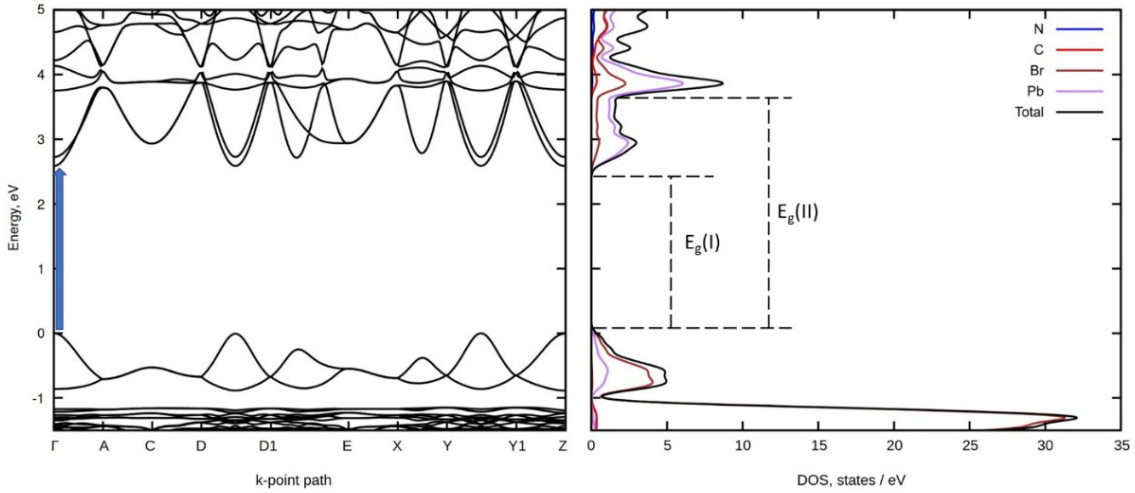

Figure S23. Electronic band structure (left) and density of states (right) for a $(C_8)DAPbBr_4$ hybrid crystal. The blue arrow indicates the electronic transition between the top of the valence band and the bottom of the conduction band.

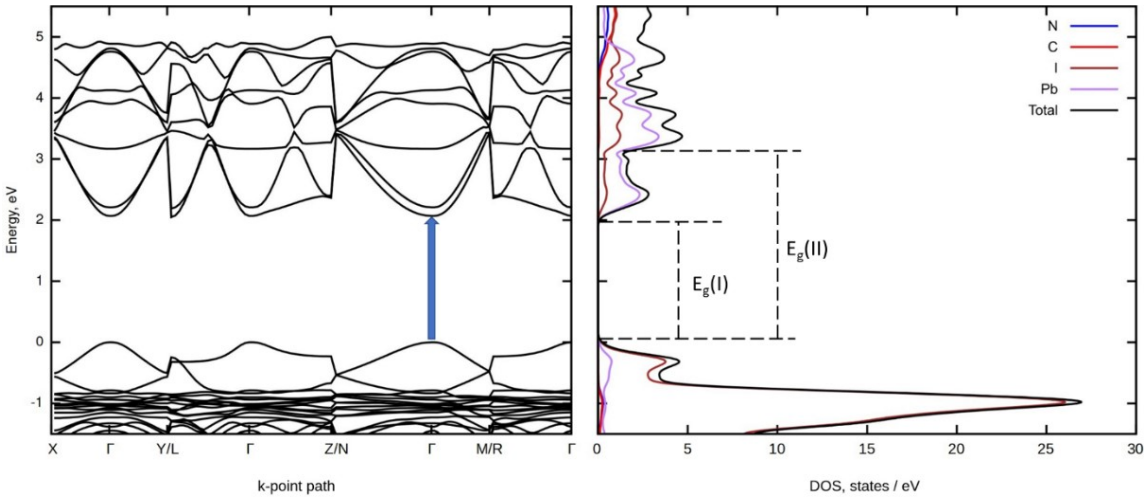

Figure S24. Electronic band structure (left) and density of states (right) for a $(C_4)DAPbI_4$ hybrid crystal. The blue arrow indicates the electronic transition between the top of the valence band and the bottom of the conduction band.

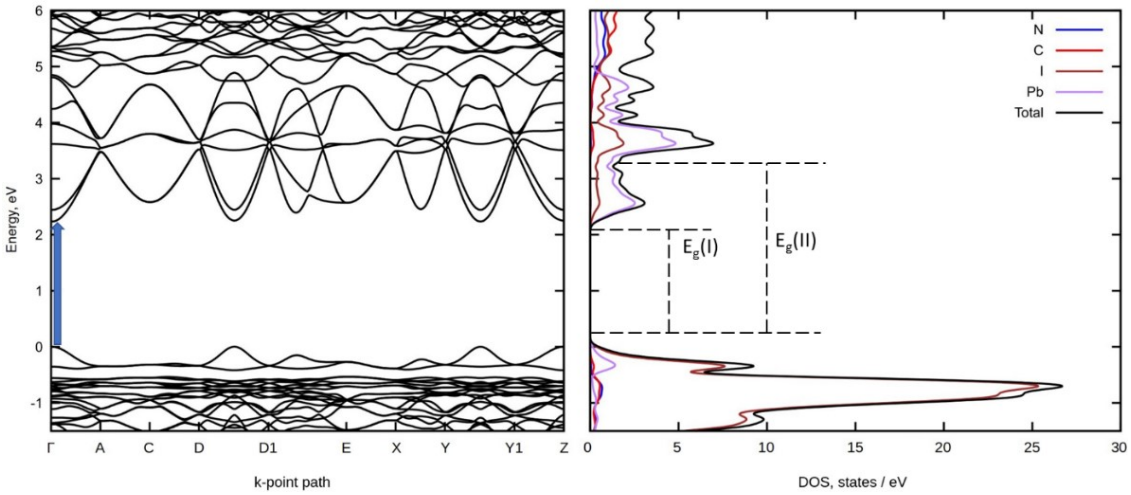

Figure S25. Electronic band structure (left) and density of states (right) for a $(C_6)DAPbI_4$ hybrid crystal. The blue arrow indicates the electronic transition between the top of the valence band and the bottom of the conduction band.

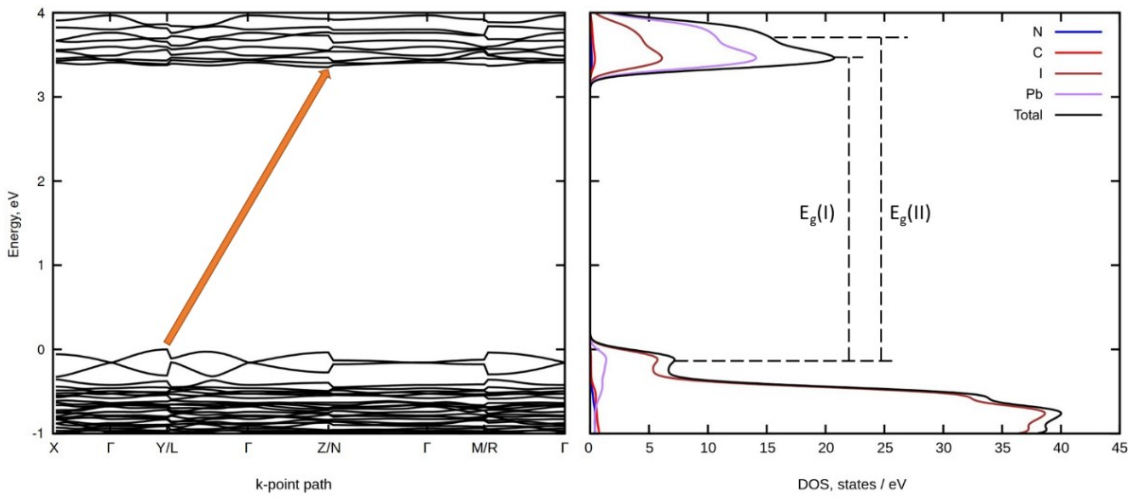

Figure S26. Electronic band structure (left) and density of states (right) for a $(C_7)DAPbI_4$ hybrid crystal. The blue arrow indicates the electronic transition between the top of the valence band and the bottom of the conduction band.

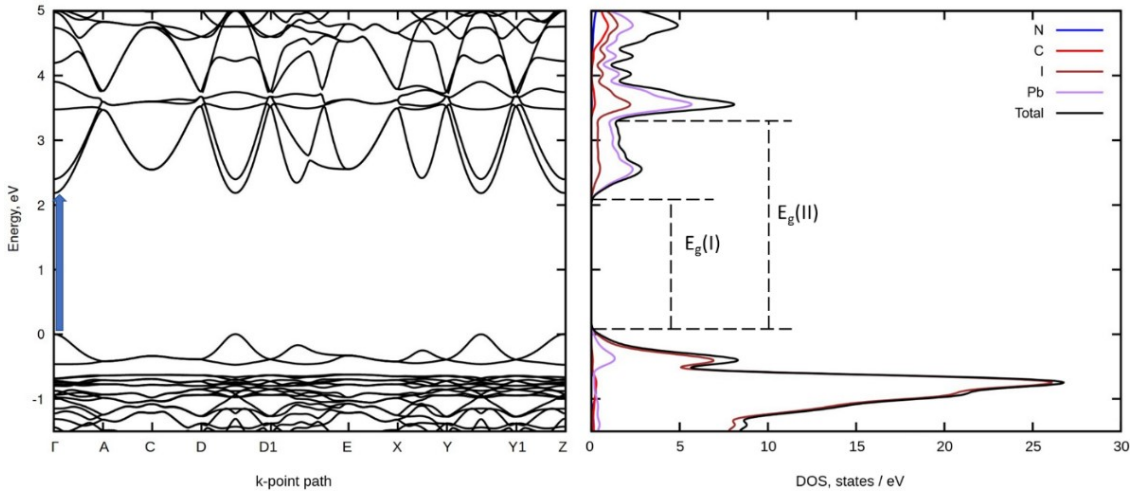

Figure S27. Electronic band structure (left) and density of states (right) for a $(C_8)DAPbI_4$ hybrid crystal. The blue arrow indicates the electronic transition between the top of the valence band and the bottom of the conduction band.

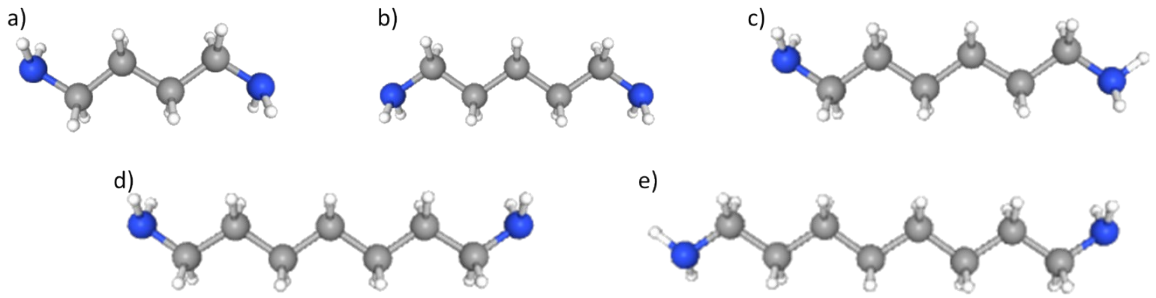

Figure S28. The structure of organic molecules acting as cations in the hybrid crystals investigated are (a) 1,4-diaminobutane (C_4DA), (b) 1,5-diaminopentane (C_5DA), (c) 1,6-diaminohexane (C_6DA), (d) 1,7-diaminoheptane (C_7DA), and (e) 1,8-diaminooctane (C_8DA).

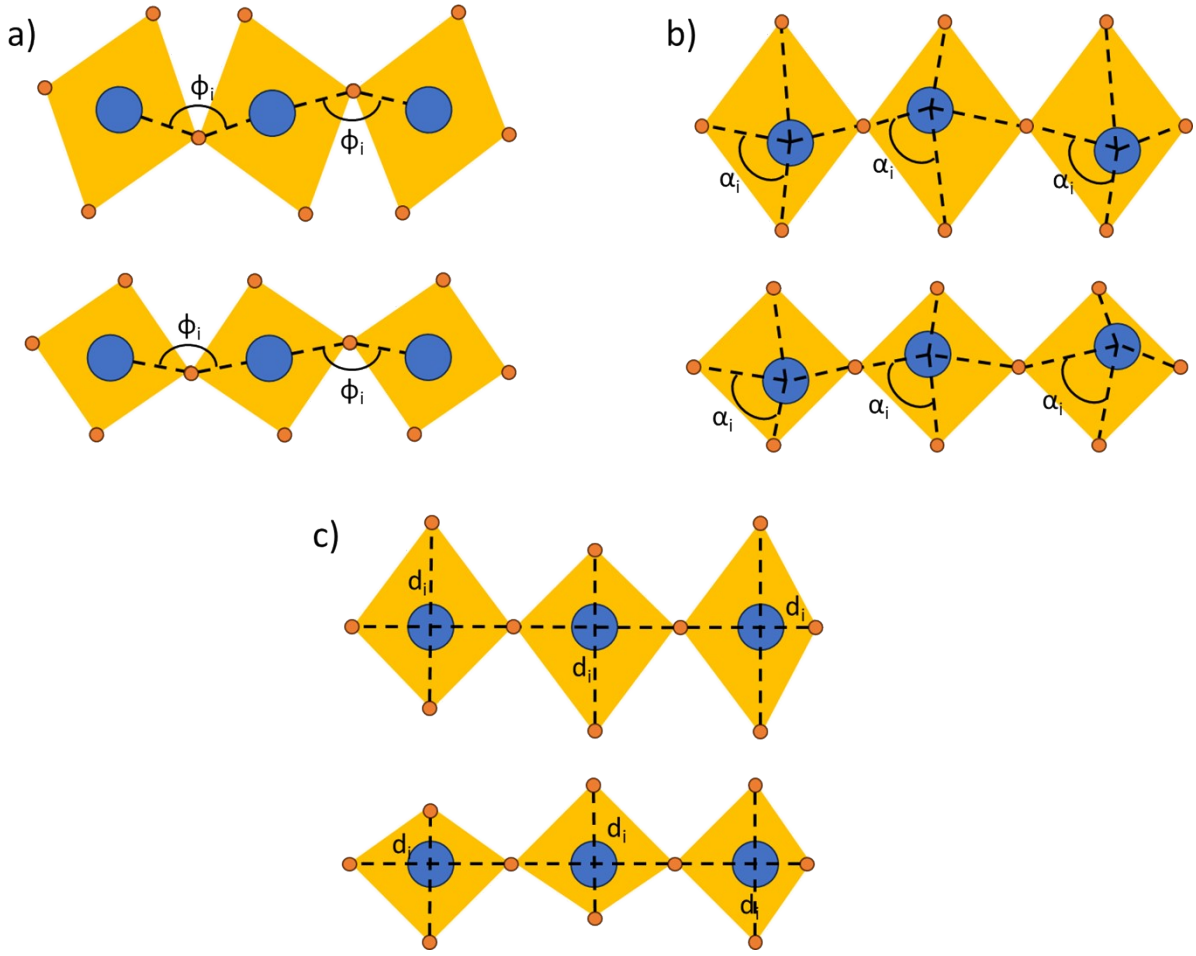

Figure S29. Disordered variants of inorganic octahedra in real crystals.